TREE CROWN DELINEATION ON UAV IMAGERY USING COMBINATION OF MACHINE LEARNING ALGORITHMS WITH MAJORITY VOTING

A. Hosingholizade[1], Y. Erfanifard[1] *, S. K. Alavipanah [1], H. Latifi [2], Y. Jouybari-Moghaddam [3]

[1] Dept. of Remote Sensing and GIS, Faculty of Geography, University of Tehran, Tehran, Iran - (a.hosingholizade, erfanifard, salavipa)@ut.a.ir
[2] Dept. of Photogrammetry and Remote Sensing, Faculty of Geodesy and Geomatics Engineering, K.N. Toosi University of Technology, Tehran, Iran - hooman.latifi@kntu.ac.ir
[3] Dept. of Surveying Engineering, Faculty of Engineering, University of Bojnord, Bojnord, Iran - jouybari@ub.ac.ir

Commission IV, WG IV/3

KEYWORDS: Majority voting, SVM, Random forest, Artificial neural network, Segmentation, Bojnord.

ABSTRACT:

Crown area is one of the key parameters in determining tree growth and an important basis for estimation of biophysical characteristics at single-tree levels in natural and man-made forests. Therefore, the present study was aimed to improve the estimation of crown area on unmanned aerial vehicle (UAV) data using a novel method in a *Pinus eldarica* man-made forest. The UAV-based RGB images with spatial resolution of 2 cm were acquired from the study area and then resampled to four pixel sizes of 10, 30, 50 and 70 cm. The resampled images were classified by three methods, i.e., Support vector machine (SVM), Random forest (RF), and Artificial neural network (ANN), which are all ensemble (bagging) classification methods. In the next step, the maps of three classification methods for each pixel size were combined by majority voting algorithm at pixel level. The results showed the robustness of ANN in all pixel sizes compared to RF and SVM. Additionally, the combination of the machine learning method by majority voting algorithms had significantly improved the accuracy of *P. eldarica* crown delineation and its area estimation on the UAV orthoimages with the investigated pixel sizes.

1. INTRODUCTION

Man-made forests have diverse cycles of ecosystems and have been developed for various purposes, including reducing pressure on natural forests and preserving valuable species (Navarro et al., 2020). These forests account for about 1% of Iran's total forests and 7.3% of its forests. They occupy the world and play an important role in reducing global climate change, conserving water resources and protecting biodiversity (Zhou and Zhang, 2020). These important roles have made it more necessary to manage and solve its challenges than ever before, which require the acquisition of quantitative and qualitative information of man-made forests. This information helps managers and planners in the field of modern forestry in formulating and planning policies that require accurate and effective measurements of parameters such as area and overall shape of crowns, especially at single tree level (Kotivuori et al., 2020). In other words, unlike traditional forestry, where the forest mass is the basis of planning, in modern forestry, single trees are the basis for planning and managing the forests. Therefore, extracting information about single trees, especially crown, is of great importance (Goodbody et al., 2017).

Crown of trees is the main place of primary production, indicating general health and yield of trees (Varo-Martínez and Navarro-Cerrillo, 2021). The shape and area of crown of each tree are among the most influential parameters for identifying and controlling the processes of photosynthesis, respiration, transpiration and management (D'Odorico et al., 2020). Various physiographic functions are performed that are vital to tree's growth and development, such as carbon dioxide uptake, light energy uptake, oxygen release, and transpiration by crown (Mokashi et al., 2021). The measurement of crown is effective for determining many quantities as well as determining the performance of tree at the stage of growth, stability and production efficiency. The dimensions of crown are closely related to leaf area and the volume of crown, which is related to the function of the photosynthetic apparatus of trees (Kalisperakis et al., 2015). Therefore, it can be a major and important predictor of tree productivity and help to grow and study it carefully. Moreover, crown area is significantly correlated with growth and biomass, and its dimensions are often used as predictors in forest ecosystems, biomass and growth models (Sharma et al., 2017). Due to changes in shape and nature of area, this trend is constantly associated with changes that require monitoring area of crown and the exact shape and trend of its changes.

The shape and area of tree crown are constantly changing for various reasons, including growth processes, age, amount of sunlight, as well as the surface microclimate of each region (Miraki et al., 2021). In fact, due to the conditions of each region, season and type of each tree, the shape of crown has a growth rate in different directions, even if they are of the same type (Wu et al., 2021). Accurate description of crown shape is also an important input in physiological models (Adeline et al., 2021) and it is very effective in correctly identifying the species and the exact position of tree. Since access to a forest area is difficult, in order to obtain information about trees such as the area of crown and the shape of trees, it is necessary to use an

* Corresponding author

accurate and economical method such as using remotely sensed data obtained by unmanned aerial vehicles (UAVs) (Gülci, 2019).

The application of UAVs in obtaining very high resolution images as well as the ability to fly at low altitudes have led to a more accurate determination of the elevation of the earth's surface, which has a great impact on the measurement of crowns. UAVs have been used in many man-made forest researches over the past few years, saving significant time, manpower and financial resources for various forest projects. Such capabilities are widely used for man-made forest monitoring plans in developing countries, where many forest monitoring plans have been done with UAV measurements, which has led to reduced maintenance costs and continuous monitoring of forest sites. It is necessary to have sufficient and continuous knowledge to apply effective methods in the correct tree identification, classification and delineation of tree crowns (Paneque-Gálvez et al., 2014).

So far, many algorithms have been developed and used for crown extraction. However, since each algorithm has its limitations in some areas, none of them can fully manage all kinds of crown extraction problems. For example, the use of algorithms such as Watershed and other common catchment-based algorithms, despite their advantages, due to low image overlap, heavy processing, inadequate DSM and DTM construction and, consequently, CHM, ground surface uncertainty, and noise have limitation. In generation of point cloud, there are limitations such as misdiagnosis of tree with other existing features, differences in methods in accurately determining the maximum point of trees. For example, the proper functioning of "Local Maxima" filter in tree location identification depends on the size, distribution, and spatial resolution of image (Wulder et al., 2000), which can inadvertently impose unrealistic results in research. The use of object-oriented methods on images with high spatial and spectral resolution can also provide a potentially efficient approach to draw a forest tree crown. However, with the abundance of information, object-oriented image classification based on image with high spatial resolution is less efficient in some cases due to high computations, manual adjustment of spectral parameters, and poor robustness. On the other hand, it is difficult to extract the shape of tree crown based only on RGB images, because in a forest, pixel values of crown are affected by sunlight and the shape of the tree. Additionally, low spatial resolution images tend to reduce the variance between pixels due to the inclusion of different types of surface coatings in each pixel. In contrast, images with high spatial resolution, such as UAV images, split the surface into smaller pixels and record more variance. As a result, it will increase the volume of processing, create close spectra and increase the number of segments in the image (Tajrin et al., 2022).

The identification of single trees on UAV data has been reported in several studies, however, the efficiency of commonly used machine learning algorithms such as Random forest (RF), Artificial neural network (ANN), Support vector machine (SVM) and Fusion methods at the decision level and the effect of different pixel sizes on their performance have less been investigated in man-made forests. Therefore, the use of different classification methods, each of which has been used separately and with a completely different approach in forest areas, and their combination with the "Majority voting" algorithm will lead to a more realistic decision, which of course needs further investigation. The results can provide a clear view of the reduction in processing volume, flight time, more appropriate altitude adjustment to further cover the area and, consequently, the reduction in the number of flight lines.

2. MATERIALS AND METHODS

2.1 Study Area

Pardisan Park is located at 8 km of Bojnord-Mashhad road in North Khorasan Province (N, Zone 40 N″57 ′28 ° 37-E″49 ′25 ° 57), adjacent to "Baba Aman" Forest Park and at an average altitude of 1080 meters above sea level (Figure 1). This complex is under the management of the General Department of Environmental Protection of North Khorasan Province in the form of a two-row fence and is purely covered with *Pinus eldarica*. The trees in this complex have been planted in two time periods in 2004 and 2010 with a distance of about 3 meters from each other. The region is cold semi-arid according to the Koppen climate classification system (Roshani et al., 2021) and has a relatively high slope in terms of topography (altitude from 1037 m to 1112 m) with average rainfall and temperature of 260 mm and 15 °C in a 10-year period (2010-2020) according to Bojnord Airport Meteorological Station (The station closest to the study area).. The main soil type of this park is silty clay and silty loam. The area of the park is about 351 hectares, of which approximately 21 hectares are covered by *P. eldarica* man-made stands. Due to the restrictions on issuing flight permits in the region, an area of approximately 14 hectares was considered for the present study.

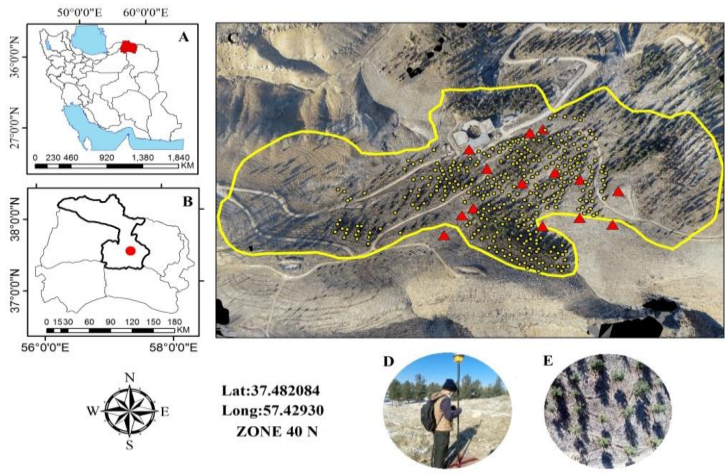

Figure 1. The study area in Iran (A), North Khorasan Province (B), Pardisan Park, red triangulation: target point, yellow point: 324 pine tree (C), Field target point (D), Orthophoto (E).

2.2 UAV imagery

In the present study, RGB images were acquired by Phantom 4 Pro UAV. The UAV has a three-axis gimbal to prevent any vibration and to balance the camera properly in various image capture missions, so that it prevents images from being captured with high tilt. The images were collected according to the type of topography at a height of 40 meters and vertically with longitudinal and transverse overlaps of 80 and 40%, respectively (Surový et al., 2018). All images were then visually reviewed to confirm no blur and light scatter at the edges of the image. Environmental conditions such as light winds with a speed of less than one Knot and clear air were also considered in selecting the flight day. The general specifications of the camera used and the digital aerial images are given in Table 1.

Items	Specifications
Camera maker	DJI
Camera model	FC6310
Focal length	24 mm
Image dimensions	3448 × 5472 Pixels
The size of each image	20 Megapixel
shutter speed	1/160 Second
Horizontal resolution	72 dpi
Vertical resolution	72 dpi
Image format	JPG
Colour combination	RGB
Saturation	Normal
Clarity	Normal
Contrast	Normal
UAV speed	4 m/s
Camera tilt control mode	Active
Positioning system	GPS/GLONASS

Table 1. Specifications of the UAV camera and digital aerial images used in the present study.

The flights were carried out on March 4, 2021 at 14:30 local time (11: 00 GMT) and a total of 952 standard and reviewed images were acquired to cover the study area. In order to georeference the images and prepare their orthomosaic, 14 ground control points were registered by a dual frequency differential global positioning system (DGPS). Ground control points were selected considering the appropriate distance of points from each other, spatial distribution within the study area along with good visibility from different directions of image were considered. In order to prevent some errors such as stretching during imaging, a speed of about 4 m/s was used (Tu et al., 2020). In this study, 39 images that did not have the necessary conditions were excluded from the process. From the remaining images after the necessary processing, the three-dimensional model was created using the Structure from Motion (SfM) algorithm.

2.3 Data processing

In this study, multiresolution segmentation method with appropriate segmentation coefficients (i.e., Scale Parameter = 25 pixels, Shape = 0.1, Compactness = 0.5 per pixel) was used to determine the crown boundary of single trees on the 2-cm colour orthoimages which was considered as the reference map. The original UAV images with 2-cm pixel size taken from the study area were resampled to pixel sizes of 10, 30, 50, 70 cm according to the range of tree crown areas. In the next step, three methods of SVM, RF and ANN, which are all in the Ensemble (bagging) category, were applied for classification of all images with mentioned four pixel sizes (i.e., each classification method was used on the images with four pixel sizes of 10, 30, 50, and 70 cm). The parameters of SVM were the radial basis function (RBF) as the kernel function, gamma of 0.33, and penalty of 100. In RF, the number of decision trees (ntree) and maximum tree depth were 50 and 30, respectively. Finally, the parameters of ANN were logistic activation function, training rate and momentum of 0.2 and 0.9, respectively, with two hidden layers and 1000 iterations. The reference data (i.e., variable number of pixels mentioned in Table 3) were divided into separate training (70%) and test (30%) datasets for all classification methods. Then all four output maps obtained by each method were converted into a single map for each pixel size by Majority voting algorithm. The algorithm involves summing the votes for class labels assigned to each pixel from the classification methods and predicting the class with the most votes for each pixel. In the final step, the four final output maps (obtained from the images with pixel sizes of 10, 30, 50, and 70 cm) were compared to the segmented 2-cm orthoimage.

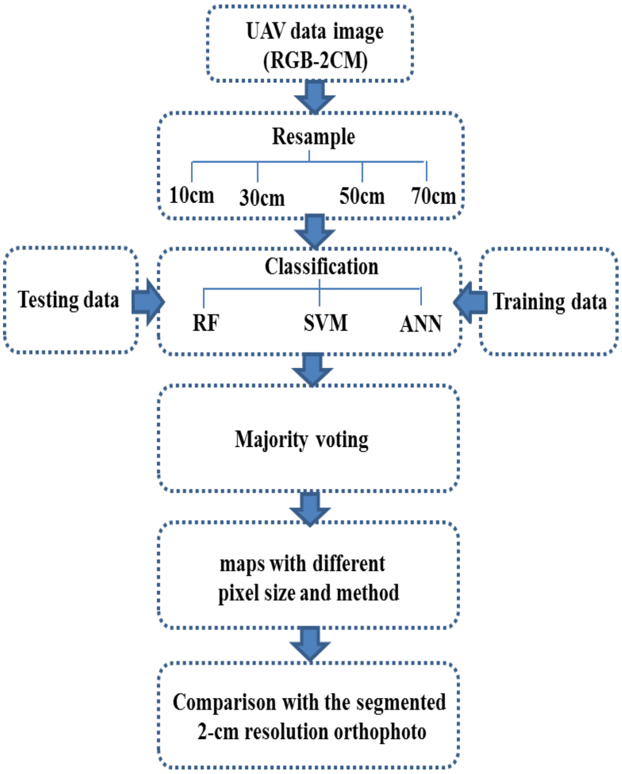

Figure 2. The flowchart of the study.

2.4 Accuracy Assessment

The parameters of sensitivity (Eq. 1), specificity (Eq. 2), accuracy (Eq. 3) and precision (Eq. 4) of target class (i.e., tree crown) were used in the present study. Specificity is the proportion of actual negatives (pixels of other classes) that are correctly identified and sensitivity (True Positive Rate) is the proportion of actual positives (pixels of the desired class) that are correctly identified. Accuracy is the proportion of true positives (pixels of the desired class) out of the total predicts (all pixels) and precision is the proportion of true positives (pixels of the desired class) out of the total predicted positives.

$$\text{Specificity} = \frac{\text{TN}}{\text{TN} + \text{FP}} \tag{1}$$

$$\text{Sensitivity} = \frac{\text{TP}}{\text{TP} + \text{FN}} \tag{2}$$

$$\text{Accuracy} = \frac{\text{TP} + \text{TN}}{\text{n}} \tag{3}$$

$$\text{Precision} = \frac{\text{TP}}{\text{TP} + \text{FP}} \tag{4}$$

where n = total number of classified pixels
TP = pixels correctly assigned to the desired class
TN = pixels not correctly assigned to the desired class
FP = pixels incorrectly assigned to the desired class
FN = pixels incorrectly assigned to the desired class

3. RESULTS AND DISCUSSION

In this study, 324 *P. eldarica* individuals with different crown areas were considered. Table 2 summarizes the estimated tree biophysical characteristics on the RGB 2-cm resolution orthoimage of the study area. The size of crown area shows the diversity of tree age in the selected individuals within the study area, however, the variation in tree height is less than crown size because of less competition for sunlight in man-made forests. Studying the sample trees with different age classes plays an important role in more effective evaluation of the algorithms in estimating the crown area of *P. eldarica* individuals. Previous studies have also emphasized the need for tree crown size diversity in comparison of UAV-based estimations and field measurements (Gu et al., 2020). Torres-Sánchez et al. (2018) studied the biophysical characteristics of 325 almond trees on UAV imagery, in which the number of sample trees was similar to the present study.

Characteristics	MIN	MAX	MEAN	STD	CV
Height (m)	38.9	2.6	6.6	13.1	0.5
Small crown diameter (m)	25.4	1.1	4.3	7.8	1.0
Large crown diameter (m)	23.4	1.4	5.8	11.6	2.3
Crown area (m^2)	49.7	7.9	15.9	49.9	0.8

Table 2. Statistical summary of the biophysical characteristics of 324 *P. eldarica* trees measured on the RGB 2-cm resolution UAV orthophoto

According to previous studies (e.g., Hosingholizade et al., 2022) and trial and error, the segmentation parameters (Scale: 25, Compactness: 0.1, Shape: 0.5) were selected to segment the RGB 2–cm resolution orthoimage of the UAV. These values had the best performance in delineation of the crown boundary of *P. eldarica* individuals in the study area compared to other values. Regarding the segmentation results, the total crown area of 324 individuals was 5556 m^2 and considered as the ground truth for accuracy assessment of the estimations. As shown in Table 2, the smallest crown size (i.e., 0.8 m^2) was covered by two pixels of the orthoimage with lowest spatial resolution investigated in this study (i.e., 70 cm). Therefore, it can be mentioned that the selected pixel sizes of the resampled images were appropriate to the crown area of *P. eldarica* individuals.

Table 3 shows the number of training pixels, test data, total crown area, sensitivity, specificity, accuracy and precision for each studied pixel size and the classification methods. Moreover, training and testing pixels should be considered equal in each pixel size so that the conditions are the same for different classification methods (Thanh and Kappas, 2017), so the training and testing data were considered the same in this study (e.g., 13650 training and 5850 test pixels for 10-cm resolution orthoimage).

The results showed the direct effect of pixel size on the accuracy of crown delineation on UAV orthoimagery, however, the majority voting algorithm significantly reduced the effects. For instance, the accuracy of crown delineation on 70-cm resolution orthoimage was significantly higher when majority voting algorithm was used and the accuracy was almost similar with 10-cm spatial resolution when the machine learning algorithms were used separately (Table 3). Additionally, processing time decreased with increasing pixel size. However, the change in pixel size with a certain ratio (from 10 cm to other sizes) has not been associated with the ratio in time change. Also, in the ANN classification method, kappa and overall accuracy were higher than RF and SVM. Of course, image analysis with the ANN took more time. As can be seen, this rate was improved by using a combination of three classification methods with the majority voting algorithm for all pixel sizes. Examination of the crown area in pixels of different sizes showed that the best case is related to the pixel size of 10 cm when using majority voting. In other words, by increasing the pixel size in all cases, the estimated area is more different from the true crown area obtained by the 2-cm resolution orthoimage**.** In general, it was concluded that the application of majority voting algorithm with three machine learning techniques on 70-cm resolution orthoimage may provide approximately similar results obtained by UAV orthoimagery with higher spatial resolution only classified by SVM and ANN methods.

As shown in Figure 3, the visual interpretation of the results indicated significant difference between the efficiency of machine learning methods on the orthoimages with similar spatial resolution. It seems that the ANN was more reliable than the two other methods, however, their combination with majority voting algorithm outperformed in delineation of the tree crowns. Moreover, the diversity of the crown properties was high on in the orthoimage with a spatial resolution of 10 cm compared to the orthoimages with pixel sizes of 30, 50 and 70 cm (in the same number of test pixels of trees) that probably caused by sunlight angel, shadow effect, direction of branches, and shape of cones. Increasing the pixel size, i.e., decreasing the spatial resolution of the orthoimage, may cause the detail (convergence of the pixels of a complication) to disappear. In other words, the lower the diversity of pixels in a complication, the better the classification under completely equal conditions (Rafieyan et al., 2013). Therefore, according to the main goals of the present work and the research problem explained, the UAV orthoimages with low resolution such as pixel size of 70 cm should be classified by a combination of machine learning methods by majority voting algorithm to effectively delineate crowns of *P. eldarica* individuals.

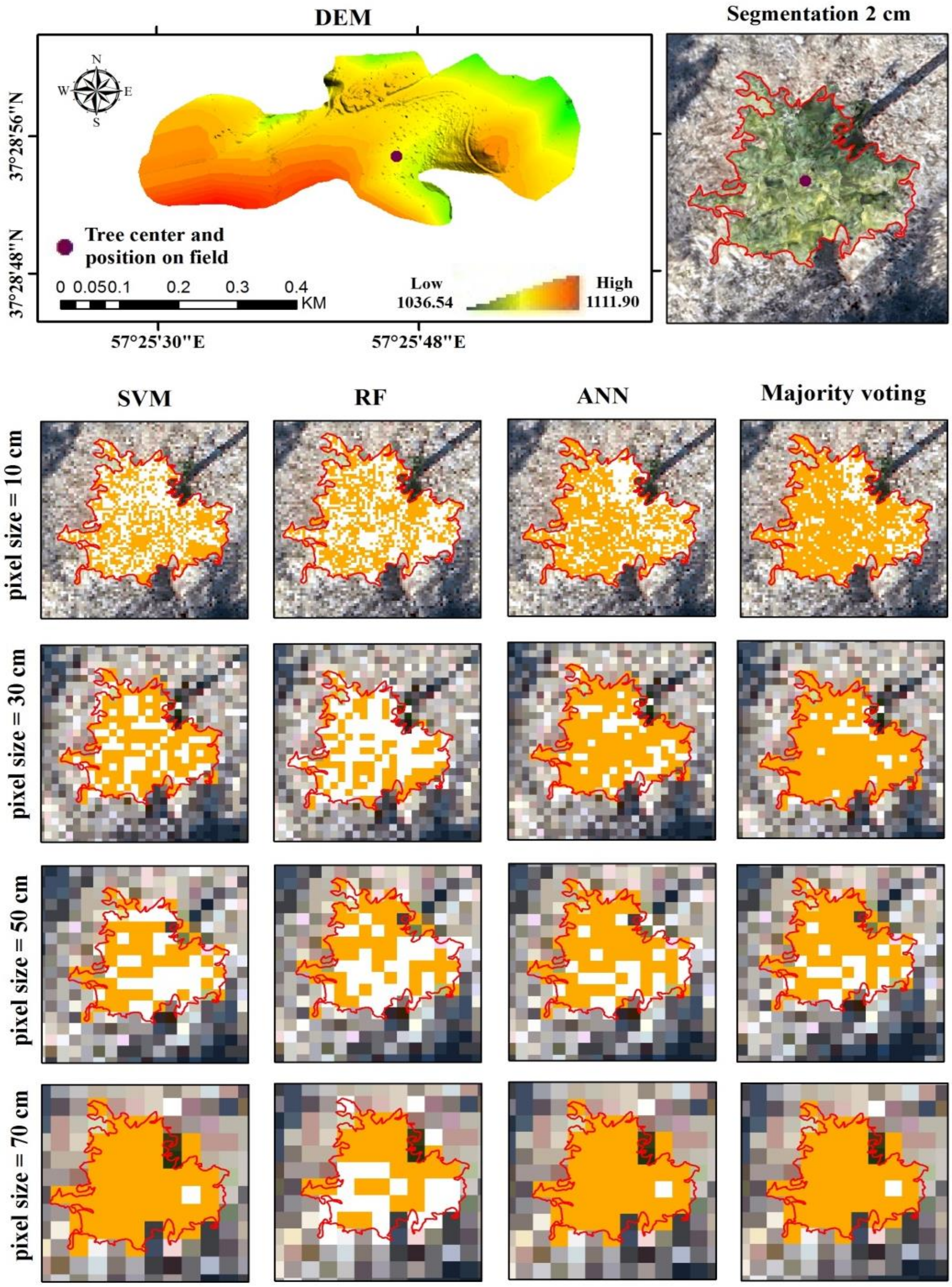

Figure 3. A part of classification results of SVM (Support vector machine), RF (Random forest) and ANN (Artificial neural network) used to delineate *Pinus eldarica* tree crowns (red polygons) on UAV orthoimages with pixel sizes of 10, 30, 50, and 70 cm. The red polygon is the true crown boundary obtained from segmentation of the 2-cm resolution orthoimage overlaid on the orthoimages with different pixel sizes for visual interpretation.

Classifier	Pixel size (cm)	Sample data (N)	Test data (N)	Total Crown Area (m^2)	Sensitivity (%)	Specificity (%)	Precision (crown) (%)	Accuracy (crown) (%)
SVM	10	13650	5850	5001	89.1	86.3	87.1	89.1
	30	4550	1950	4791	86.3	83.5	82.7	85.4
	50	2730	1170	4259	79.8	72.4	73.4	76.2
	70	1951	836	3875	74.2	71.5	71.6	75.5
RF	10	13650	5850	4876	83.4	81.1	83.9	84.8
	30	4550	1950	4689	78.5	76.8	78.6	79.2
	50	2730	1170	4211	71.8	70.9	71.8	76.4
	70	1951	836	3508	60.2	57.1	62.5	64.4
ANN	10	13650	5850	5073	92.3	89.3	89.2	92.7
	30	4550	1950	4873	87.7	85.2	88.6	89.8
	50	2730	1170	4551	83.8	79.6	83.1	86.6
	70	1951	836	4192	81.4	76.8	76.4	81.1
Majority voting	10	13650	5850	5152	94.5	92.4	94.9	96.3
	30	4550	1950	5075	92.9	90.5	92.5	94.8
	50	2730	1170	4687	89.1	82.4	88.1	91.4
	70	1951	836	4514	84.7	80.5	83.7	86.1

Table 3. Statistical summary of the crown area estimated on UAV orthoimagery with different pixel sizes

4. CONCLUSIONS

This study proposed a procedure to optimize the efficiency of commonly used machine learning methods (i.e., SVM, RF and ANN) by their combination with majority voting algorithm for crown delineation of *P. eldarica* individuals on UAV orthoimagery. Moreover, the effect of pixel size on the performance of the methods was investigated. The results revealed the robustness of the suggested process and the crowns of the trees were well separated from other features. The investigated approach provided approximately similar results on the 70-cm resolution orthoimagery compared to application one machine learning method on very high resolution orthoimage, i.e., the pixel size of 10 cm. The procedure applied in this study can help scientists use this technique to classify low resolution UAV-based orthoimages or even other high relation satellite-based remotely sensed data sets. It also should be mentioned that an intensive and time-consuming field work is necessary to determine the boundaries of tree crowns, while the crown boundaries delineated on the 2-cm resolution orthoimage was used as the ground truth in the present study that can be considered in future studies.

ACKNOWLEDGEMENTS

The authors are grateful to the General Directorate of Environmental Protection of North Khorasan Province. Additionally, the research was financially supported by the project number 4003393 funded by Iran National Science Foundation (INSF).

REFERENCES

Adeline, K.R., Briottet, X., Lefebvre, S., Rivière, N., Gastellu-Etchegorry, J.P., and Vinatier, F., 2021. Impact of tree crown transmittance on surface reflectance retrieval in the shade for high spatial resolution imaging spectroscopy: A simulation analysis based on tree modeling scenarios. *Remote Sens.*, 13(5), 931-965.

Alok, A. K., Saha, S., and Ekbal, A., 2016. Multi-objective semi-supervised clustering for automatic pixel classification from remote sensing imagery. *Soft Comput.*, 20(12), 4733-4751.

Belgiu, M., and Drăguţ, L., 2016. Random forest in remote sensing: A review of applications and future directions. *ISPRS J. Photogramm. Remote Sens.*, 114, 24-31.

D'Odorico, P., Besik, A., Wong, C. Y., Isabel, N., and Ensminger, I., 2020. High-throughput drone-based remote sensing reliably tracks phenology in thousands of conifer seedlings. *New Phytol.*, 226(6), 1667-1681.

Goodbody, T.R., Coops, N.C., Marshall, P.L., Tompalski, P., and Crawford, P., 2017. Unmanned aerial systems for precision forest inventory purposes: A review and case study. *For. Chron.*, 93(1), 71-81.

Gu, J., Grybas, H. and Congalton, R.G., 2020. Individual tree crown delineation from UAS imagery based on region growing and growth space considerations. *Remote Sens*., 12, 2363.

Gülci, S., 2019. The determination of some stand parameters using SfM-based spatial 3D point cloud in forestry studies: an analysis of data production in pure coniferous young forests. *Environ. Monit. Assess.*, 191, 1-17.

Hosingholizade, A., Erfanifard, Y., Alavipanah, S.K., Latifi, H., and Jouybari-Moghaddam, Y., 2022. Comparison of unmanned aerial vehicle (UAV) RGB imagery and point clouds in crown area estimation of individual trees within pine (*Pinus eldarica*) man-made forests. *RS and GIS for Natural Resources*. https://girs.bushehr.iau.ir/article_689615.html. [In Persian]

Kalisperakis, I., Stentoumis, C.H., Grammatikopoulos, L., and Karantzalos, K., 2015. Leaf area index estimation in vineyards from UAV hyperspectral data, 2D image mosaics and 3D canopy surface models. *The International Archives of Photogrammetry, Remote Sensing and Spatial Information Sciences*, 40(1), 299.

Kotivuori, E., Kukkonen, M., Mehtätalo, L., Maltamo, M., Korhonen, L., and Packalen, P., 2020. Forest inventories for small areas using drone imagery without in-situ field measurements. *Remote Sens. Environ.,* 237, 111404.

Miraki, M., Sohrabi, H., Fatehi, P., and Kneubuehler, M., 2021. Individual tree crown delineation from high-resolution UAV images in broadleaf forest. *Ecol. Inform.,* 61, 101207.

Mokashi, M.V., Ghatanatti, S.M., and Mutanal, S.M., 2021. Oxygen productivity in different tree species. *Indian J. Ecol.,* 48(2), 373-375.

Navarro, A., Young, M., Allan, B., Carnell, P., Macreadie, P., and Ierodiaconou, D., 2020. The application of UAVs to estimate above-ground biomass of mangrove ecosystems. *Remote Sens. Environ.,* 242, 111747.

Paneque-Gálvez, J., McCall, M. K., Napoletano, B. M., Wich, S. A., and Koh, L. P., 2014. Small drones for community-based forest monitoring: An assessment of their feasibility and potential in tropical areas. *Forests,* 5(6), 1481-1507.

Rafieyan, O., and Darvishsefat, A.A., 2014. The effect of spatial and radiometric resolutions of aerial images for tree species classification by object-based approach. *Iranian Journal of Forest and Poplar Research,* 22(1), 121-132. [In Persian]

Roshani, A., Parak, F., and Esmaili, H., 2021. Trend analysis of climate change compound indices in Iran. *J. Water Clim. Chang.,* 12, 801-816.

Shao, Y., and Lunetta, R.S., 2012. Comparison of support vector machine, neural network, and CART algorithms for the land-cover classification using limited training data points. *ISPRS J. Photogramm. Remote Sens.,* 70, 78-87.

Sharma, R.P., Bílek, L., Vacek, Z., and Vacek, S., 2017. Modelling crown width–diameter relationship for Scots pine in the central Europe. *Trees*, 31(6), 1875-1889.

Šiljeg, A., Panđa, L., Domazetović, F., Marić, I., Gašparović, M., Borisov, M., and Milošević, R., 2022. Comparative assessment of pixel and object-based approaches for mapping of olive tree crowns based on UAV multispectral imagery. *Remote Sens.,* 14(3), 757.

Surový, P., Almeida Ribeiro, N., and Panagiotidis, D., 2018. Estimation of positions and heights from UAV-sensed imagery in tree plantations in agrosilvopastoral systems. *Int. J. Remote Sens.,* 39, 4786-4800.

Syazwani, R.W.N., Asraf, H.M., Amin, M.M.S., and Dalila, K.N., 2022. Automated image identification, detection and fruit counting of top-view pineapple crown using machine learning. *Alex. Eng. J.,* 61(2), 1265-1276.

Tajrin, T., Ahmed, M., and Zaman, S., 2022. Detection of lung cancer stages on computed tomography image using laplacian filter and marker controlled watershed segmentation technique. *Period. polytech. Electr. Eng. Comput. sci.,* 66(2), 105-115.

Thanh Noi, P., and Kappas, M., 2017. Comparison of random forest, k-nearest neighbor, and support vector machine classifiers for land cover classification using Sentinel-2 imagery. *Sensors,* 18(1), 18.

Torres-Sánchez, J., de Castro, A.I., Pena, J.M., Jimenez-Brenes, F.M., Arquero, O., Lovera, M., and Lopez-Granados, F., 2018. Mapping the 3D structure of almond trees using UAV acquired photogrammetric point clouds and object-based image analysis. *Biosyst. Eng.,* 176, 172-184.

Tu, Y.H., Phinn, S., Johansen, K., Robson, A., and Wu, D., 2020. Optimizing drone flight planning for measuring horticultural tree crop structure. *ISPRS J. Photogramm. Remote Sens.,* 160, 83-96.

Varo-Martínez, M., and Navarro-Cerrillo, R.M., 2021. Stand delineation of *Pinus* plantations suffering decline processes based on biophysical crown variables. *Remote Sens.,* 13, 436.

Vivar-Vivar, E.D., Pompa-García, M., Martínez-Rivas, J.A. and Mora-Tembre, L.A., 2022. UAV-Based characterization of tree-attributes and multispectral indices in an uneven-aged mixed conifer-broadleaf forest. *Remote Sens*., 14, 2775.

Wu, S., Wang, J., Yan, Z., Song, G., Chen, Y., Ma, Q., and Wu, J., 2021. Monitoring tree-crown scale autumn leaf phenology in a temperate forest with an integration of PlanetScope and drone remote sensing observations. *ISPRS J. Photogramm. Remote Sens.,* 171, 36-48.

Wulder, M., Niemann, K.O., and Goodenough, D.G., 2000. Local maximum filtering for the extraction of tree locations and basal area from high spatial resolution imagery. *Remote Sens. Environ*., 73, 103-114.

Zhou, X., and Zhang, X., 2020. Individual tree parameters estimation for plantation forests based on UAV oblique photography. *IEEE Access,* 8, 96184-96198.